FLAGELLAR HYDRODYNAMICS

A Comparison between Resistive-Force Theory and Slender-Body Theory

R. E. Johnson, *Department of Engineering Science, and*
C. J. Brokaw, *Division of Biology, California Institute of Technology, Pasadena, California 91125 U.S.A.*

ABSTRACT This paper investigates the accuracy of the resistive-force theory (Gray and Hancock method) which is commonly used for hydrodynamic analysis of swimming flagella. We made a comparison between the forces, bending moments, and shear moments calculated by resistive-force theory and by the more accurate slender-body theory for large-amplitude, planar wave forms computed for a flagellar model. By making an upward empirical adjustment, by about 35%, of the classical drag coefficient values used in the resistive-force theory calculations, we obtained good agreement between the distributions of the forces and moments along the length of the flagellum predicted by the two methods when the flagellum has no cell body attached. After this adjustment, we found the rate of energy expenditure calculated by the two methods for the few typical test cases to be almost identical. The resistive-force theory is thus completely satisfactory for use in analysis of mechanisms for the control of flagellar bending, at the current level of sophistication of this analysis. We also examined the effects of the presence of a cell body attached to one end of the flagellum, which modifies the flow field experienced by the flagellum. This interaction, which is not considered in resistive-force theory, is probably insignificant for small cell bodies, such as the heads of simple spermatozoa, but for larger cell bodies, or cell bodies that have large-amplitude motions transverse to the swimming direction, use of slender-body theory is required for accurate analysis.

INTRODUCTION

The resistive-force theory developed for flagellar hydrodynamics in the pioneering work of Gray and Hancock (1955) has been extensively used in subsequent studies of flagellar propulsion and the generation of flagellar bending (cf. Brokaw, 1965, 1970, 1972; Blum and Lubliner, 1973). Propulsive velocities predicted by resistive-force theory have been verified experimentally, but no direct experimental verification of the power dissipation and the distribution of moments along a flagellum, predicted by resistive-force theory, has been possible. Models for controlling the active shear moment generated within a flagellum have now increased in sophistication to the point where it is appropriate to ask whether the predictions of resistive-force theory are sufficiently accurate for use in studying internal flagellar mechanics.

The underlying assumption of resistive-force theory is that the hydrodynamic forces are

---

Dr. Johnson's present address is Department of Theoretical and Applied Mechanics, University of Illinois at Urbana-Champaign, Urbana, Ill. 61801.

Biophys. J. © Biophysical Society · 0006-3495/79/01/113/15 $1.00
Volume 25 January 1979 113-127

proportional to the local body velocity, with the constant of proportionality being defined as the force (or drag) coefficient. As pointed out by Lighthill (1976), this assumption is inconsistent with the true hydrodynamic situation in which viscous effects dominate and produce long-range hydrodynamic interactions. These interactions can, for discussion purposes, be divided into two categories: (*a*) flagellum-flagellum interactions, and (*b*) cell body-flagella interactions. The flow field actually experienced by a point moving with the flagellum will be influenced by (*a*) the configuration and movement of all other parts of the flagellum, and especially by the proximity of the ends of the flagellum, and (*b*) by the position and movement of a cell body attached to one end of the flagellum. Attempts at compensating for the effects of (*a*) have been made in previous studies by the use of drag coefficients that depend on the wavelength of the flagellar bending waves (Hancock, 1953; Gray and Hancock, 1955; Brokaw, 1965; Lighthill, 1976). Lighthill (1976) made a preliminary analysis of cell body-flagella interactions.

These long-range interactions can be evaluated accurately by the hydrodynamic theory that we call the slender-body theory. Application of slender-body theory to flagellar hydrodynamics has been attempted previously by Hancock (1953), Lighthill (1976), and Shen et al. (1975). Further improvements in slender-body theory (Wu, 1976, 1977; Johnson, 1977) have led to methods that can be routinely applied to calculations for flagellar propulsion, although they still require more extensive numerical computation than the methods based on resistive-force theory. In this paper we present the results calculated using both resistive-force theory and slender-body theory for the distributions of forces, bending moments, and shear moments along the length of a flagellar model generating typical planar bending waves, so that a direct comparison of the predictions of these two theories can be made. Our objective is to identify those situations in which the simpler resistive-force theory can be used without misleading our efforts to understand the mechanisms that control active shear moment in flagella.

METHODS

Resistive-Force Theory (RFT)

In the classical RFT the force/length, **f**, exerted on the fluid by the flagellum at a point s (s being the arc length along a flagellum) is proportional to the local center line velocity $\mathbf{V}(s, t)$ (in a coordinate frame in which the fluid is at rest at infinity). Separating **V** into components lying along the directions normal and tangential to the body center line, V_n, V_s respectively, we have the corresponding two components of the force/length,

$$f_s = \mu C_s V_s, \quad f_n = \mu C_n V_n. \tag{1}$$

Note that we have separated out the fluid viscosity, μ, in Eq. 1 to make the force coefficients dimensionless. The frequently used coefficients proposed by Gray and Hancock (1955) for computing flagellar motions are

$$C_s = \frac{2\pi}{\ln \frac{2\lambda}{b} - \frac{1}{2}}, \quad \gamma = \frac{C_n}{C_s} = 2, \tag{2}$$

where b is the cross-sectional radius of the flagellum and λ the wavelength. The ratio, $\gamma = 2$, given by Gray and Hancock is only correct for the limiting case of a vanishingly thin flagellum. Brokaw

(1975) suggested, on the basis of Cox's results (1970), that a more appropriate value for C_n was

$$\frac{4\pi}{\ln \frac{2\lambda}{b} + \frac{1}{2}}$$

which, for a sea urchin spermatozoon, should give $\gamma = 1.7$. However, best agreement with experimental measurements was obtained when using $\gamma = 1.8$ (Brokaw, 1970) and for this reason, this value was used in subsequent work (Brokaw, 1972*a*). Lighthill (1976) considered the case of a simple flagellum performing planar bending waves of small amplitude and helical waves of arbitrary amplitude, while producing zero net thrust (a flagellum without cell body drag to overcome). For these cases Lighthill's expressions for the force coefficients are

$$C_s = \frac{2\pi}{\ln \frac{2q}{b}}, \quad C_n = \frac{4\pi}{\ln \frac{2q}{b} + \frac{1}{2}}, \tag{3}$$

where $q = 0.09\ \Lambda$ (Λ being the wavelength measured along the center line of the flagellum, or L in Brokaw's notation, 1965). Lighthill also suggested that the same values might be used for planar bending waves of arbitrary amplitude.

For a typical bending wave of a sea urchin sperm flagellum (Brokaw, 1965) Lighthill's expressions yield $\gamma = 1.8$ and $C_s = 1.58$, the latter of which is about 40% greater than the value of C_s given by Eq. 2. For comparison, in our initial computations with the resistive force theory, we used $\gamma = 1.8$ and $C_s = 1.14$, as given by Eq. 2 when $b/\lambda = 0.005$.

When applying RFT, the effects of a cell body at the basal end of the flagellum were accounted for by the conventional method, which includes the usual Stokes drag for a sphere of radius a, $6\pi\mu a\mathbf{V}_h$, where $\mathbf{V}_h$ is the cell body velocity.

Slender-Body Theory (SBT)

The general SBT to be applied here has been summarized by Wu (1976, 1977) and developed in detail by Johnson (1977). The solution of the problem of Stokes flow resulting from the motion of a slender body is constructed using the singularity method. The body is taken to be of circular cross-section, with radius $b(s)$, and is assumed to be spheroidal near the ends. The calculations for flagella were first carried out by assuming, for simplicity of numerical details, that the unbent cross-sectional form of the body was that of a prolate spheroid. This choice is quite acceptable for the present purpose since flagella are extremely slender ($\epsilon = b/l$ is typically 0.005, where l is the half-length of the flagellum) with the cross-sectional area varying slowly along its length. It is not the cross-sectional area variation of the flagellum but its motion of large amplitude that is expected to be the principal factor in generating the flow fields. In fact, only minor differences were found between the results obtained with this approximation and with a flagellum of constant cross-section fitted smoothly to prolate spheroidal ends.

The application of SBT leads to an integral equation for the force per unit length, $\mathbf{f}$, acting on the fluid by an arbitrary three-dimensional slender body, of which the center line is given by $\mathbf{x}(s, t)$. This equation is given in detail in the Appendix. The present analysis is limited to motions in a plane. This integral equation was solved for each specific time, t, at which $\mathbf{x}(s, t)$ and $\mathbf{V}(s, t)$ are specified, by applying a quadratic quadrature formula to the integral term in the integral equation to produce a linear algebraic system. The linear system was then solved for $\mathbf{f}$ by applying the Gauss-Seidel iteration method. Details of the solution technique and tests on a straight, slender prolate spheroid, for which a well-known analytical solution is available, and on a slender torus, for which an analytic closed form solution was recently obtained, have been given elsewhere (Johnson, 1977; Wu and Johnson, 1976). These tests showed that five significant figure accuracy was obtained with only 20 space divisions along the length of the body.

The integral equation also includes the hydrodynamic interaction effects between cell body and flagellum. For that case the SBT has been modified (Johnson, 1977) to include the long-range velocity field disturbance produced by the presence of a cell body. In that analysis the method introduced by Burgers (1938) was used to satisfy an approximate no-slip boundary condition on a cell body surface with an attached flagellum. Although cell bodies come in a variety of shapes, our calculations were carried out for a spherical cell body. This should be sufficient to give an approximate indication of the effects produced by a cell body of given size, and allow an exact comparison between the effects predicted by RFT, which neglects such interactions, and SBT.

Wave Form Data

Unfortunately, no available data for actual flagella contain velocity information of sufficient accuracy for these calculations. A simple sinusoidal bending wave of constant amplitude is unsatisfactory for these calculations because it does not correctly represent the reduced amplitude of oscillation as characteristically found near the basal end of real flagella. Instead we used data generated by a flagellar model (Brokaw, 1972*a*) that simulates the behavior of a flagellum that generates bending waves by an active shear system controlled by the curvature of the flagellum. The bending waves generated by this model exhibit the main characteristics typical of real flagellar waves, although they do not exactly duplicate the behavior seen near the ends of real flagella. The flagellar model is divided into 32 intervals along its length, and the computations generate a motion that exactly balances the active, viscous, and elastic bending moments at each "joint" between segments, using RFT in the computation of the viscous moments resulting from the fluid resistance. The model contains internal viscous and elastic resistances; for the present computations, linear elastic resistances were used, and the nonlinearity required for stabilization at a particular amplitude was introduced by using an expression for the active moment that is slightly different from that used originally (Brokaw, 1972*a*). The active shear moment, m, which is equal to $-\mathrm{d}M_A/\mathrm{d}s$, where M_A represents the resulting active bending moment, is obtained from

$$\tau \frac{\mathrm{d}m}{\mathrm{d}t} = \frac{m_0 \kappa}{|\kappa| + \kappa_0} - m \tag{4}$$

where κ is the curvature of the flagellum and κ_0 is a value of curvature which gives $m = m_0/2$. For these calculations, $\kappa_0 = 0.0001$ rad/nm. The time constant, τ, and maximum shear moment, m_0, describe the active shear system for this model.

Wave form data were generated by using the methods described previously (Brokaw, 1972*a*), using 32 time steps per beat cycle. Positions and velocities for wave forms at five equally spaced time points covering one half of a beat cycle were then used for computations of forces, bending moments, and shear moments (equal to $-\mathrm{d}M/\mathrm{d}s$), by both RFT and SBT for comparison. Representative results are presented for two time points at one fourth beat cycle apart.

The hydrodynamic bending moment and shear moment for planar wave forms are calculated from (see Appendix for details on notation),

$$M(s) = -\mathbf{e}_b \cdot \left\{ \mathbf{R}_h \times \mathbf{f}_h + \int_{-l}^{s} \mathbf{R}_0(s') \times \mathbf{f}(s') \mathrm{d}s' \right\}, \tag{5}$$

$$m(s) = -\frac{\mathrm{d}M}{\mathrm{d}s} = \mathbf{e}_b \cdot \left\{ \mathbf{e}_s(s) \times \left[\mathbf{f}_h + \int_{-l}^{s} \mathbf{f}(s') \mathrm{d}s' \right] \right\}, \tag{6}$$

where $-l$ is the basal end of the flagellum. The rate at which mechanical energy is expended by the flagellum in overcoming the viscous drag is

$$P = \int_{-l}^{l} \mathbf{f} \cdot \mathbf{V} \, \mathrm{d}s \tag{7}$$

RESULTS

Flagellum without a Cell Body

The first wave form to be analyzed is illustrated in Fig. 1 *a*. The parameters used to generate this wave form are listed in Table I, using notation consistent with Eq. 4 and with Brokaw (1972*a*). The wavelengths (λ and Λ) used in obtaining the force coefficients for RFT are not well defined for these wave forms, but approximate values are sufficient since these parameters appear in the logarithmic term, and minor variations do not significantly affect the force coefficients. The normal and tangential force per unit length, the bending moment, M, and the shear moment, $m = -\mathrm{d}M/\mathrm{d}s$, were calculated by RFT and SBT and are compared in Fig. 2 at two time points in the beat cycle.

At all time points examined, both the net force, ($= \int_{-l}^{l} \mathbf{f}(s)\mathrm{d}s$), and the total moment, M, at the distal end of the flagellum ($s = l$), are found to be negligible with both the RFT and SBT calculations. This result is expected for the RFT calculation, since RFT and the free swimming condition of zero net force and moment at the end of the flagellum are used in computing the motion of the flagellar model. Obtaining the same result with the SBT calculation suggests that the value of $\gamma = 1.8$ used for the RFT provides here an excellent agreement with the SBT results.

The results in Fig. 2 suggest that the primary difference between the RFT and SBT calculations is in the magnitude of the forces and moments per unit length, while the distributions along the length of the flagellum are very similar. This suggests that the fundamental assumption of RFT, that the local force/length is proportional to the local velocity, may be

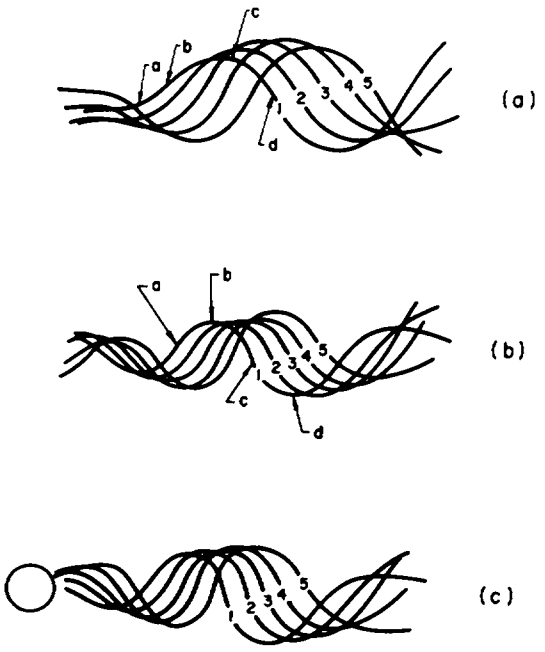

FIGURE 1 Flagellar beat patterns during half a cycle generated using the parameters given in Table I; case *a* and *b* are headless, cell body radius in case *c* is 2 μm.

TABLE I

PARAMETERS USED TO GENERATE WAVE FORMS

	Fig. 1*a*	1*b*	1*c*
Freq, s^{-1}	30.0	53.2	43.0
$2l$, μm	40.0	40.0	40.0
b, μm	0.1	0.1	0.1
λ, μm	20.0	12.5	12.5
Λ, μm	32.0	20.0	20.0
a, μm	0.0	0.0	2.0
Model parameters*			
E_S	8.0	5.0	5.0
E_B	0.80×10^8	0.44×10^8	0.44×10^8
C_B	0.12×10^7	0.33×10^6	$.33 \times 10^6$
C_S	0.0	0.0	0.0
τ	0.40×10^{-2}	0.20×10^{-2}	0.20×10^{-2}
m_0	40.0	30.0	25.0

*Dimensions of model parameters are consistent with Brokaw (1972*a*) and are given here in piconewtons, nanometers, and seconds.

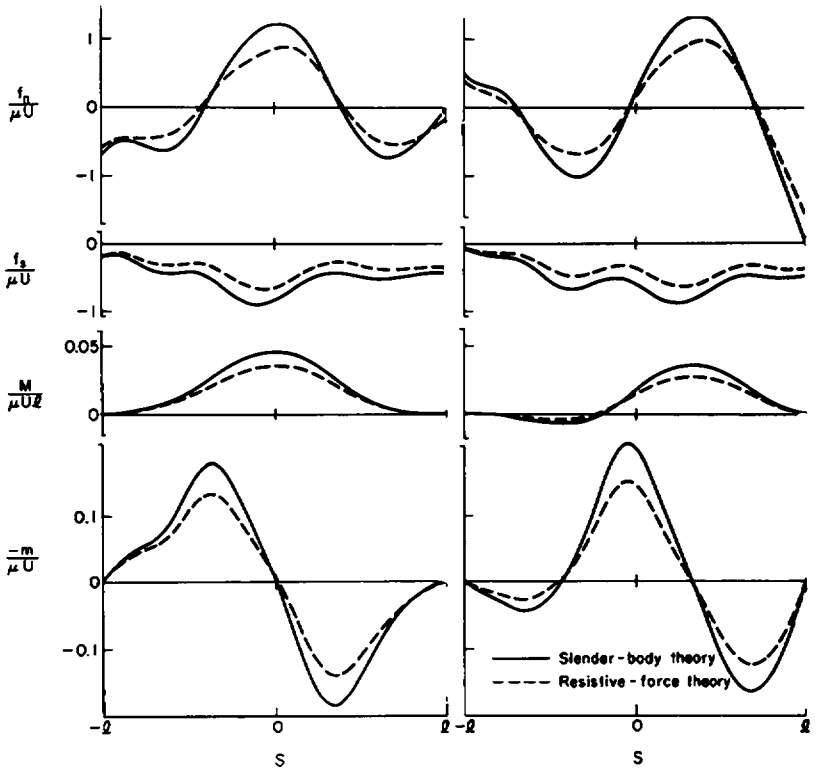

FIGURE 2 Force/length, moment, and shear moment for time instants 1 (left) and 3 (right) shown in Fig. 1 *a* (characteristic velocity U = freq. × l).

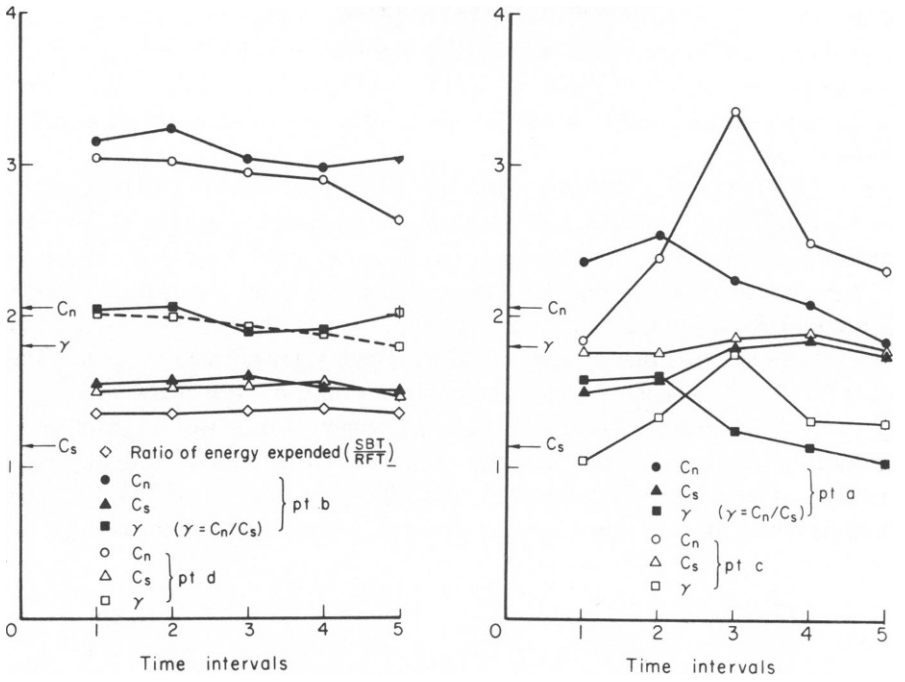

FIGURE 3 The force coefficients for the points *a*, *b*, *c* and *d* which move with the wave indicated in Fig. 1 *a*. Arrows indicate constant Gray and Hancock coefficients. Also shown is ratio of energy expended by flagellum.

satisfactory, but that more accurate values for the force coefficients are required. Fig. 3 shows the force coefficients defined by $C_\nu = f_\nu/\mu V_\nu$, $\nu = n, s$, which can be obtained from the SBT calculations. They are plotted as functions of time for the four phase points, *a*, *b*, *c*, and *d*, indicated in Fig. 1 *a*, that are moving with the wave. Points *a* and *c* correspond to points of maximum curvature, i.e., wave peaks, and *b* and *d* are points of minimum curvature, i.e., the relatively straight regions between peaks. Planar wave forms generate their thrust in the minimum curvature or straight regions while drag is produced at the wave peaks. The arrows in Fig. 3 indicate the value of the constant Gray and Hancock coefficients.

For the minimum curvature or thrusting regions the C_n predicted by SBT varies in time by at most 15%, while C_s varies only slightly. We see that the Gray and Hancock coefficients underestimate the C_n of SBT in this region by 25–50%, while C_s is underestimated by roughly 30%. For points at the wave peaks, C_s varies only moderately with time, while the variations in C_n are rather erratic and become as large as 45%. At these maximum curvature points the Gray and Hancock coefficients are in error by from 10 to 60%. The large variations of C_n with time at the wave peaks may be expected because at those points the RFT hypothesis fails. It fails because the center line velocity, V_n, can become small at some time instants, with the induced fluid velocities produced by flagellar-flagellar interactions becoming a dominant factor in producing the force/length on the body. As an estimate of the dependence of the force coefficients on arc length, *s*, we note that a comparison between the minimum and maximum curvature points indicates that variations of 20%

are not uncommon. Consequently, to obtain a high degree of accuracy, arc-length-dependent force coefficients would be required for finite amplitude planar wave forms. Furthermore, we note that the ratio $\gamma = 1.8$ is found to fall between the value at the wave peaks and straight regions and is therefore a reasonable average value, being clearly better than a value of two.

In terms of RFT, the rate of energy expended by the flagellum (Eq. 7) depends linearly on the drag coefficients, and therefore the ratio of this quantity calculated by RFT and SBT serves as a useful average value estimate (with respect to arc length) of the accuracy of the RFT force coefficients. In Fig. 3 we observe that the Gray and Hancock coefficients consistently underestimate the rate of energy expended in the present case by approximately 35%. This suggests that an approximate average value correction to the Gray and Hancock RFT due to flagellar-flagellar interactions would be to increase the drag coefficients by 35%. With such an increase in the hydrodynamic forces we can produce a wave form identical to that in Fig. 1 by increasing the model parameters E_B, E_S, and m_0 by an equal amount. Comparison between RFT and SBT after such a correction to the force coefficients produces the results in Fig. 4 for the same wave form and time instants just dis-

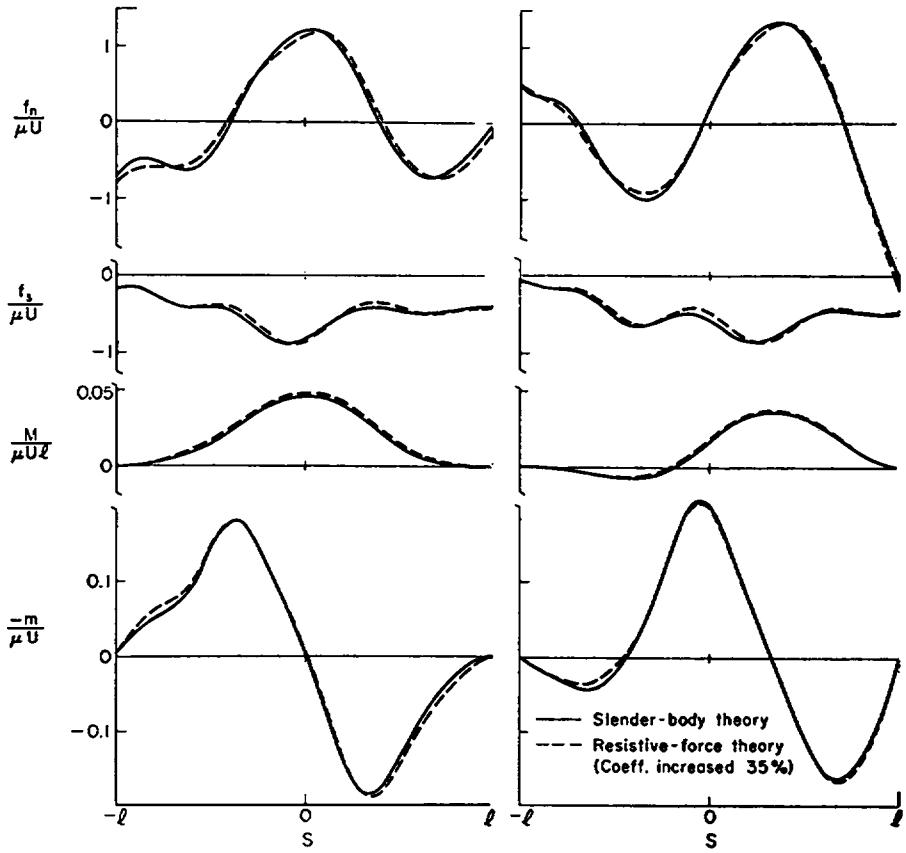

FIGURE 4 Force/length, moment, and shear moment for time instants 1 and 3 shown in Fig. 1*a* (characteristic velocity U = freq. × l).

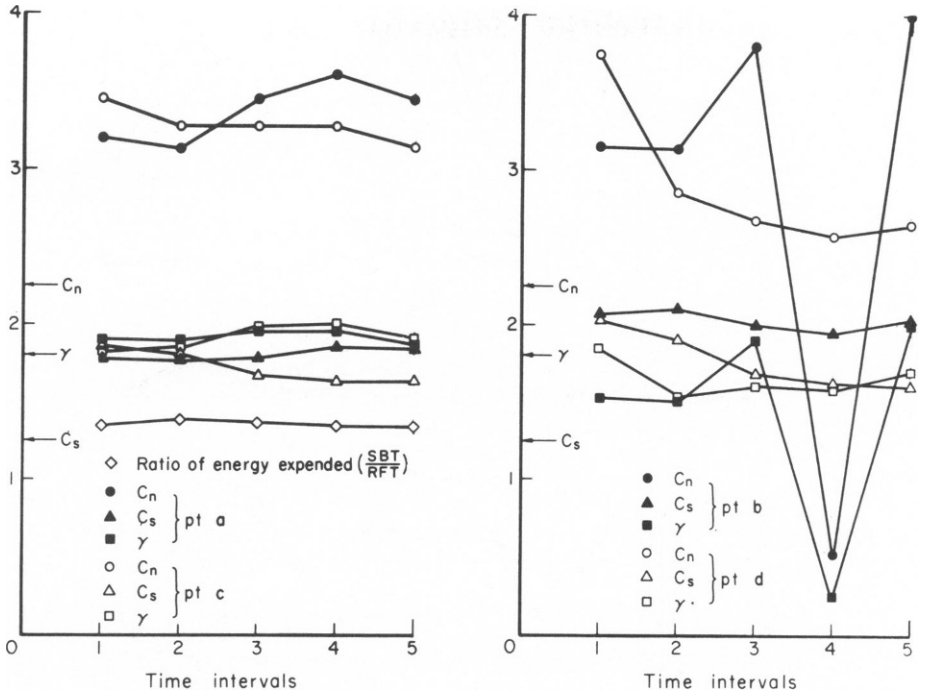

FIGURE 5 The force coefficients for the points *a*, *b*, *c* and *d* which move with the wave indicated in Fig. 1*b*. Arrows indicate constant Gray and Hancock coefficients. Also shown is ratio of energy expended by flagellum.

cussed. It is rather remarkable that such a crude average value modification of the Gray-Hancock coefficients produces such good agreement between the two theories. We observe that the forces are slightly out of phase, with the most significant differences in the forces and shear occurring near the body ends, whereas the error in the moment is nearly uniform.

The wave form in Fig. 1 *a* was chosen to be representative of wave forms commonly found on spermatozoa such as sea urchin spermatozoa. A second wave form, shown in Fig. 1 *b*, was generated with slightly modified parameters to give a wave form with greater curvatures and shorter wavelengths, which might be expected to increase the flagella-flagella interactions. Calculations of the force coefficients from SBT, as in Fig. 3, are shown in Fig. 5. As in the previous example, the ratio of the energy expenditures calculated by SBT and RFT again suggests that an increase in the Gray-Hancock drag coefficients by 35% would yield the best results with the modified RFT calculations. After making this adjustment, the forces and moments calculated by the two methods are compared in Fig. 6. In this case also, the modified RFT calculation gives a close approximation to the more accurate SBT results.

Flagellum with a Cell Body

The presence of a spherical cell body, having a radius of 2 μm, attached to the basal end of a flagellum having properties similar to the case in Fig. 1 *b*, produced the wave motion illustrated in Fig. 1 *c*. In this case, and in other cases we examined, a small net moment was obtained from the SBT calculations at the distal end of the flagellum, as shown in Fig. 7.

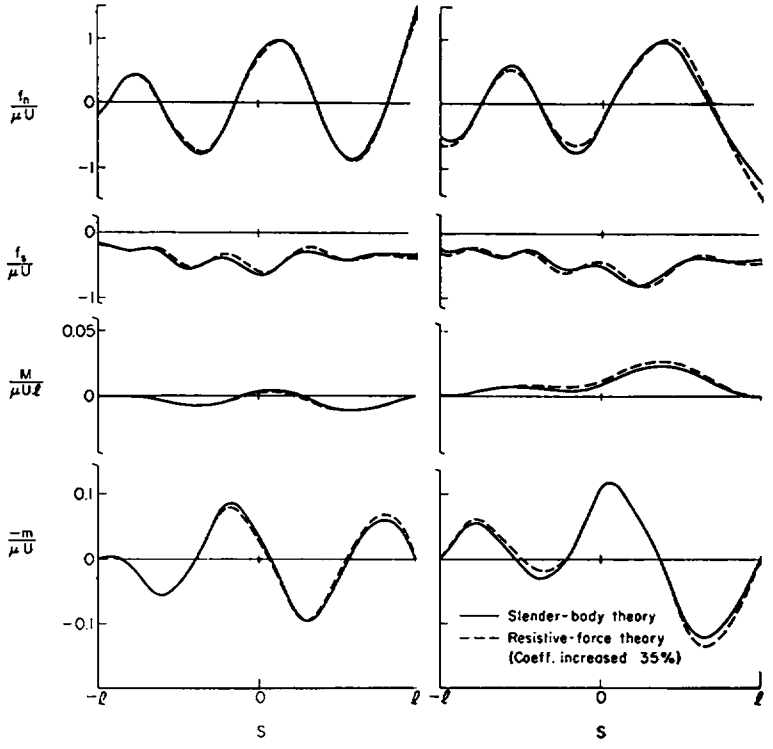

FIGURE 6 Force/length, moment, and shear moment for time instants 2 and 4 shown in Fig. 1*b* (characteristic velocity U = freq. × l).

This means that the RFT calculation, which neglects the cell body-flagellum interactions, does not provide correctly the swimming velocity and trajectory when a cell body is present.

One of the interaction effects is due to the presence of a force distribution along the flagellum that generates a net thrust to overcome the cell body drag. Such a flagellar force distribution has a long-range hydrodynamic influence, inducing a local flow field in the neighborhood of the cell body and consequently altering the forces experienced by the cell body from that of Stokes drag on a sphere moving similarly in the absence of a flagellum. In Fig. 8 we compare the two cell body forces, one determined with, and the other without, the inclusion of cell body interactions. Two cases are shown, one being the wave form in Fig. 1 *c* and the other being a flagellar motion very similar to that in Fig. 1 *a*, both with a typical cell body radius of 2 μm. F_x is the force component in the swimming direction and F_y is in the transverse direction. Variations in the ratios in Fig. 8 are found to be much larger for F_y than for F_x. This is because the force in the swimming direction (F_x) is dominated by the steady swimming velocity, being less sensitive to the fluid motion induced by the flagellum. The actual cell body force calculated by SBT contributes to the non-zero net moment seen in Fig. 7.

Further, a certain amount of fluid is dragged along by the cell body, which alters the force generated by the flagellum. This interaction effect will be the strongest for points of the flagellum nearest the cell body. In the present case this variation is most clearly seen

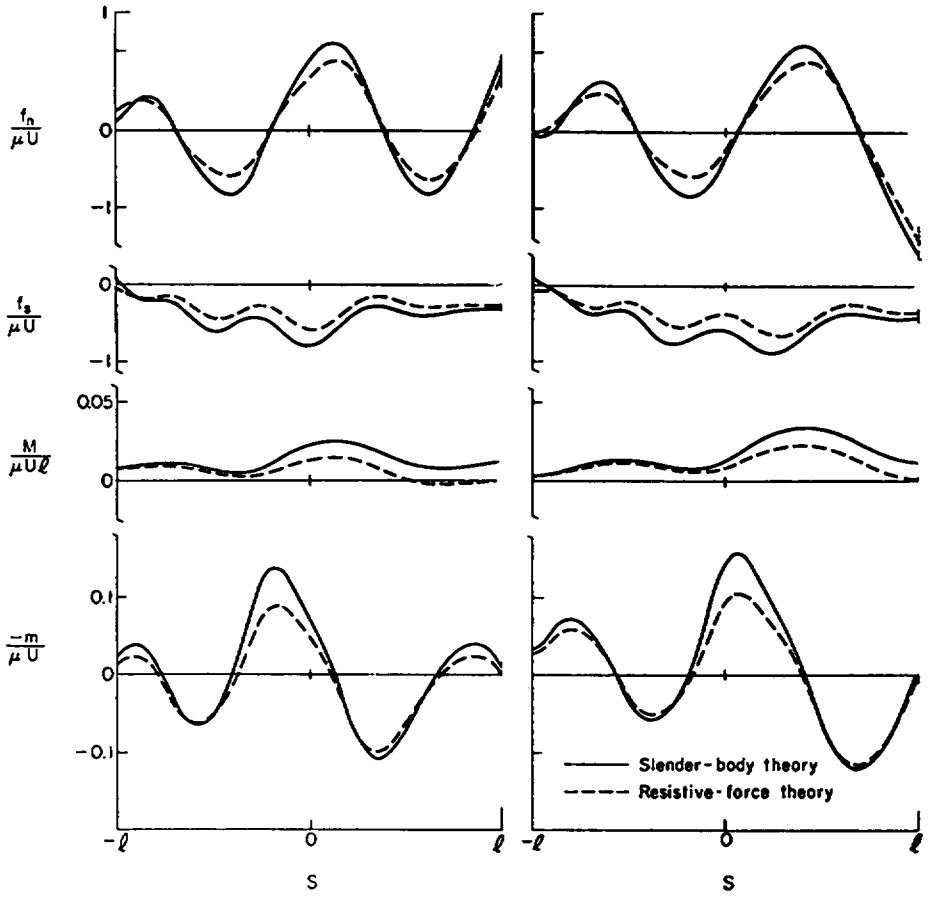

FIGURE 7 Force/length, moment, and shear moment for times instants 2 and 4 shown in Fig. 1*c* (characteristic velocity U = freq. × l).

(Fig. 7) near $s = -l$, where the tangential fluid velocity incident on the flagellum is decreased by the presence of the cell body, producing a displacement of the tangential force/length in a positive sense. This interaction effect should not be overlooked when considering the accurate modeling of the basal end of the flagellum, especially for flagella having high curvatures near the cell body or for organisms with large cell bodies.

For the cases possessing a cell body, the rate of energy expended by the flagellum alone was found to be 30–32% greater when calculated by SBT than by Gray and Hancock theory. This is very similar to that found in the headless case. Here, however, a simple increase in the drag coefficients of the flagellum alone is not sufficient to produce good agreement between RFT and SBT, since deviation in the cell body forces and flagellar forces near the cell body lead to differences in the hydrodynamic bending moment.

DISCUSSION

Beginning with the work of Machin (1958), efforts to understand the mechanisms responsible for generation of bending waves by flagella have focused on a search for mechanisms

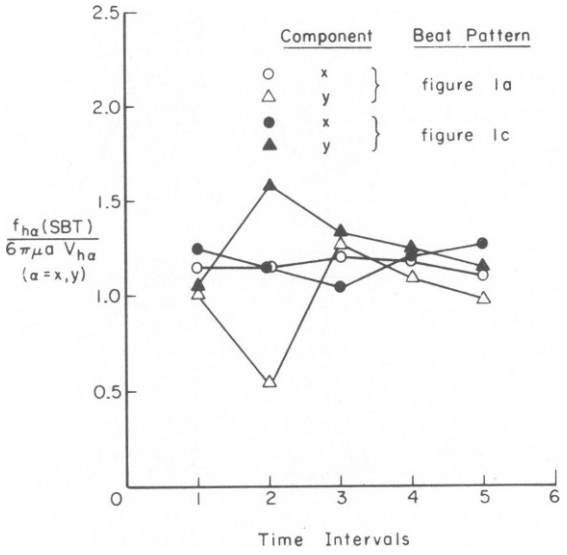

FIGURE 8 Ratio of cell body force including interactions, $f_{h\alpha}(\alpha = x, y)$, to the force neglecting interactions, i.e., Stokes drag $(6\pi\mu a\, V_h)$.

for controlling the active moment generated within a flagellum. The motion of the flagellum represents the solution of a moment balance equation (actually a fourth order nonlinear partial differential equation) that balances the active moment, moments resulting from the elasticity of flagellar structures, and moments resulting from viscous resistances to movement of the flagellum. Evidence that the active process in flagella and cilia involves an active sliding displacement of flagellar microtubules (reviewed by Brokaw, 1972*b*) led to an emphasis on the active shear moment, $m(s)$, as an important variable (Brokaw, 1970; Rikmenspoel, 1971). A specific proposal for a control mechanism in which active shear moment is proportional to flagellar curvature was considered in detail (Brokaw, 1970, 1972*a*), and was found to be sufficient to give spontaneous initiation and propagation of bending waves on a model flagellum. However, the conclusions of that analysis were completely dependent on the use of RFT in describing the distribution of viscous moments along the length of the flagellum.

Our present analysis of flagellar motion, using both RFT and SBT, indicates that the more accurate treatment of flagellar hydrodynamics provided by SBT does not alter the principal conclusions obtained by RFT. The shear moment distributions calculated by SBT and RFT are sufficiently similar to ensure that the successful simulation of flagellar movement by the model of Brokaw (1972*a*) would also be possible using SBT, and that the present differences between the simulated movements and the movements of real flagella result from limitations of the model rather than limitations of the hydrodynamic analysis.

Previous applications of RFT to flagellar hydrodynamics have also provided estimates of the magnitudes of the shear moments and energy expenditure generated by flagella. These need to be revised upward by about 35% for consistency with SBT. For example, measurements of the metabolism of actively swimming *Ciona* spermatozoa by Brokaw and

Benedict (1968) led to an estimate of 7–8 kJ of viscous work output per mole of ATP used; this estimate should now be revised upwards to 10–11 kJ/mol.

For the finite amplitude planar beat patterns examined here, Lighthill's coefficients (Eq. 3), which were derived for finite amplitude helical wave forms, produced results almost indistinguishable from those obtained using the increased Gray and Hancock coefficients (Figs. 4 and 6). Apparently Lighthill's coefficients incorporate the average value effects of flagellar-flagellar interactions and therefore are convenient for obtaining more accurate results.

When a cell body is present, the RFT with the increased Gray and Hancock coefficients produces reasonably accurate results for the force/length experienced by the flagellum. However, accurate determination of the cell body forces, necessary in balancing the net forces and moments, is not obtained by the RFT, and requires a proper accounting of the interaction effects. Although Lighthill's coefficients are not valid for the thrusting case, they give good agreement for the flagellar forces between RFT and SBT when a cell body is present.

It appears from the results presented here that whenever the effect of a cell body is significant it will be necessary to use the SBT to account accurately for the hydrodynamic interactions. Incorporation of SBT into the models which simulate flagellar movement will be necessary for analysis of these cases. However, in the absence of a cell body, or for small cell bodies such as those of sea urchin spermatozoa, it is sufficient in practical application to employ RFT since the computational effort required to use SBT outweighs the additional accuracy gained.

The authors with to thank Professor Theodore Y. Wu for his many helpful suggestions during the preparation of this paper.

This investigation was jointly supported by the Biomedical Research Support Grant Program, Division of Research Resources, National Institute of Health (Grant RR07003), the National Institute of Health (Grant GM21931 to CJB), the National Science Foundation (Grant ENG 74-23008), and the Office of Naval Research (Contract N0014-76-C-0157).

Received for publication 3 July 1978.

APPENDIX

The integral equation derived by Johnson (1977) which determines the force/length, $\mathbf{f}$, exerted on the fluid by a flagellum which may in general have a three dimensional centerline and the force exerted on the fluid by the cell body, $\mathbf{f}_h$, is given by

$$8\pi\mu V_\nu(s,t) - U_\nu(\mathbf{R}_h;\mathbf{f}_h) = \mathbf{f}_\nu L_\nu + \int_{-s_0}^{s_0} K_\nu(\mathbf{R}_0;\mathbf{f})\,ds' \qquad \text{(A)}$$

$$(\text{no sum}, \nu = n, s, b)$$

where,

$$L_s = 2(2L - 1), \quad L_n = L_b = 2L + 1,$$

$$L = \ln[2(l^2 - s^2)^{1/2}/b(s)],$$

$$K_\nu(\mathbf{R}_0;\mathbf{f}) = f_\nu(s',t)/R_0 + (\mathbf{f}(s',t)\cdot\mathbf{R}_0)R_{0\nu}/R_0^3 - D_\nu f_\nu(s,t)/|s-s'|,$$

$$D_s = 2, \quad D_n = D_b = 1,$$

$$\mathbf{R}_0 = \mathbf{x}(s,t) - \mathbf{x}(s',t) = R_{0s}\mathbf{e}_s + R_{0n}\mathbf{e}_n + R_{0b}\mathbf{e}_b,$$

$$R_0 = |\mathbf{R}_0|,$$

$$\mathbf{f}(s,t) = f_s\mathbf{e}_s + f_n\mathbf{e}_n + f_b\mathbf{e}_b,$$

$$s_0 = l(1-\epsilon^2)^{1/2},$$

where $\mathbf{e}_s$, $\mathbf{e}_n$, $\mathbf{e}_b$ are the tangential, normal, and binormal unit vectors of the flagellum center line at s where $V_\nu(s,t)$, $\nu = n, s, b$, is specified and the cell body induced flow term is given by,

$$U_\nu(\mathbf{R}_h;\mathbf{f}_h) = f_{h\nu}/R_h + (\mathbf{f}_h\cdot\mathbf{R}_h)R_{h\nu}/R_h^3,$$

$$\mathbf{R}_h = \mathbf{x}(s,t) - \mathbf{x}_h(t), \quad R_h = |\mathbf{R}_h|,$$

$$\mathbf{f}_h = 6\pi\mu a\mathbf{V}_h - \mathbf{f}',$$

$$\mathbf{f}' = \frac{3}{4}a\int_{-s_0}^{s_0}\mathbf{H}(\mathbf{R}_h;\mathbf{f})\,ds',$$

$$\mathbf{H}(\mathbf{R}_h;\mathbf{f}) = \mathbf{f}/R_h(1 + a^2/3R_h^2) + (\mathbf{f}\cdot\mathbf{R}_h)\mathbf{R}_h/R_h^3(1 - a^2/R_h^2),$$

with $\mathbf{x}_h$ being the position vector to the center of the cell body and $\mathbf{V}_h$ the cell body velocity.

The integral Eq. A determines the force/strength, $\mathbf{f}$, along the entire length of the flagellum, including the ends, with an error of order ϵ^2, where $\epsilon = b/l \ll 1$. The cell body induced flow term has derived using the method introduced by Burgers (1938) and the reader is referred to Johnson (1977) for the details. In general Eqs. A are three coupled integral equations for $f_\nu(\nu = n, s, b)$. However, in the present applications, the motion is planar, i.e. $V_b \equiv 0$, and therefore the integral equation with $\nu = b$ decouples from the remaining two equations, $\nu = s, n$ and has the trivial solution $f_b \equiv 0$. Also note that in the absence of a cell body $\mathbf{f}_h = 0$ and consequently the second term on the left hand side of Eq. A is omitted.

REFERENCES

BLUM, J. J., and J. LUBLINER. 1973. Biophysics of flagellar motility. *Annu. Rev. Biophys. Bioeng.* **2**:181.

BROKAW, C. J. 1965. Non-sinusoidal bending waves of sperm flagella. *J. Exp. Biol.* **43**:155.

BROKAW, C. J., and B. BENEDICT. 1968. Mechanochemical coupling in flagella. II. Effects of viscosity and thiourea on metabolism and motility of Ciona spermatozoa. *J. Gen. Physiol.* **52**:283.

BROKAW, C. J. 1970. Bending moments in free-swimming flagella. *J. Exp. Biol.* **53**:445.

BROKAW, C. J. 1972*a*. Computer simulation of flagellar movement. I. Demonstration of stable bend propagation and bend initiation by the sliding filament model. *Biophys. J.*, **12**:564.

BROKAW, C. J. 1972*b*. Flagellar movement: a sliding filament model. *Science (Wash. D.C.)*. **178**:455.

BROKAW, C. J. 1975. Spermatozoan motility: a biophysical survey. *Biol. J. Linn. Soc.* **7**:423.

BURGERS, J. M. 1938. On the motion of small particles of elongated form in a viscous liquid. Chap. III of second report on viscosity and plasticity. Proc. K. Ned. Akad. Wet. **16**:113.

COX, R. G. 1970. The motion of long slender bodies in a viscous fluid. Part I. General theory. *J. Fluid Mech.* **44**: 791.

GRAY, J., and G. T. HANCOCK. 1955. The propulsion of sea-urchin spermatozoa. *J. Exp. Biol.* **32**:802.

HANCOCK, G. J. 1953. The self-propulsion of microscopic organisms through liquids. *Proc. R. Soc. Lond.* (*A*): *Math. Phys. Sci.* **217**:96.

JOHNSON, R. E. 1977. Slender-body theory for Stokes flow and flagellar hydrodynamics. Ph.D. Thesis. California Institute of Technology, Pasadena, CA.

LIGHTHILL, J. 1976. Flagellar hydrodynamics. *Soc. Ind. Appl. Math.* Rev., **18**:161.

MACHIN, K. E. 1958. Wave propagation along flagella. *J. Exp. Biol.* **11**:446.

RIKMENSPOEL, R. 1971. Contractile mechanisms in flagella. *Biophys. J.* **11**:446.

SHEN, J. S., P. Y. TAM, W. J. SHACK, and T. J. LARDNER. 1975. Large amplitude motion of self-propelling slender filaments at low Reynolds numbers. *J. Biomech.* **8**:229.

WU, T. Y. 1976. Hydrodynamics of swimming at low Reynolds numbers. Symposium. 'Bewegungsphysiologie-Biomechanik.' October 1976 at the Akademie der Wissenschaften, Mainz, West Germany.

Wu, T. Y. 1977. Flagellar and cilia hydrodynamics. 1977 Biomechanics Symposium, Yale University, June 15–17, 1977.

WU, T. Y., and R. E. JOHNSON. 1976. Hydrodynamics of low-Reynolds-number flow. Part 5. Motion of a slender torus. Caltech report, ES 76-1 Eng. Sci. Dept., California Institute of Technology, Pasadena, Calif.